ACS Macro Letters

Letter

pubs.acs.org/macroletters

Flattening of Dendrimers from Solutions onto Charged Surfaces

P. M. Welch,* C. F. Welch, and N. J. Henson

Theoretical and Materials Science and Technology Divisions, Los Alamos National Laboratory, Los Alamos, New Mexico 87544, United States

Supporting Information

ABSTRACT: The adsorption of dendrimers onto charged surfaces plays a role in many emerging applications. Numerous studies found in the literature report that dendrimers flatten at these interfaces. Here, we provide a simple scaling theory that describes the height of the adsorbed layer, the fraction of segments within the dendrimer that touch the surface, and the total number of dendrimers adsorbed as a function of generation of growth, surface charge density, and concentration. We demonstrate that these predictions agree well with extensive molecular dynamics simulations. Combined, the simulations and scaling argument indicate that simultaneous adsorption and compression at the interface take place.

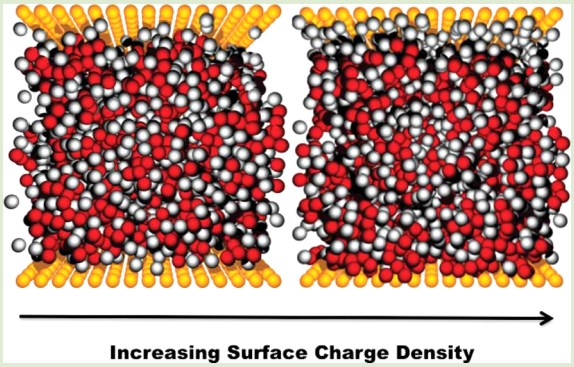

A growing list of potential biomedical[1] and nanotechnological[2] applications of dendrimers makes study of their behavior at charged interfaces particularly interesting. The behavior of linear chains near charged surfaces has been extensively investigated over the past several decades, and much is understood.[3] However, one expects that the compact, highly branched structure of dendrimers and attendant higher charge densities conspire to produce phenomenology that differs from linear analogues. In the dilute solution limit, for example, one expects that the extent that a dendrimer may stretch out to lay down on a surface varies with generation and does not generally occur to the same extent as comparably sized coils of linear chains.[4] In the concentrated regime, further variations away from the behavior of linear chains may be expected since dendrimers do not appear to interpenetrate to any appreciable extent. Many essential questions remain open regarding not only the necessary conditions for dendritic molecules to adsorb onto surfaces but also their deformation and layer structure. We lack a complete understanding of how surface concentration grows as a function of the attractiveness of the substrate, how the double layer structure changes with varying surface charge density, and the extent to which the molecule's conformation is perturbed due to the surface when other dendrimers are present. These and related questions have received much attention in both the theoretical[5−9] and experimental[10−20] literature. Answering these questions would impact not only the myriad potential applications of dendrimers but also the use of related materials such as colloids. From these studies, the following picture emerges: (i) there is a critical combination of environmental, molecular, and surface properties that exist in order for adsorption to take place; (ii) upon adsorption to a weakly attracting surface, the conformation of individual dendrimers is little perturbed; and (iii) severe deformation and flattening occur at higher attractive strengths.

This latter feature, though surprising, garners broad support from the experimental literature. For example, many reflectivity and scanning probe microscopy studies show that, on an attractive surface, the thickness of individual dendrimers and of dendrimer monolayers is smaller than the dendrimer's diameter.[10,11,13,15,16] Using ellipsometry and FTIR-external reflection spectroscopy, Tokuhisa et al.[14] further suggest that the dendrimer conformation at the surface and its resulting monolayer thickness can be manipulated by changing the dendrimer−surface interaction enthalpy relative to that of the dendrimer solution. Similarly, several groups varied dendrimer charge density to tune monolayer thicknesses.[18−20]

The primary difficulty in analytically capturing the compression of the dendrimers lies in addressing the intra- and intermolecular interactions, in addition to the impact of the charged surface on the dendrimers. Scaling theories have been successfully applied to describe individual dendrimers.[21] However, as noted by Kröger,[22] there are limitations to the applicability of scaling to dendritic molecules and their internal interactions.

In an effort to circumvent some of these difficulties and gain insight into the molecular processes active upon docking with the surface, we herein develop a simple model that is an extension of the analysis due to de Gennes[23,24] for ideal linear chains. To carry out this analysis, we must first build an effective ideal model for dendrimers that accounts for the swelling of the molecule due to intramolecular interactions. We previously proposed a recipe for constructing such a model.[25] As in similar treatments of linear chains, the key element lies in

Received: October 15, 2013
Accepted: January 21, 2014
Published: January 28, 2014

dx.doi.org/10.1021/mz400524c | ACS Macro Lett. 2014, 3, 180−184

rescaling the step length between segments to capture the intramolecular repulsions that drive the squared radius of gyration R_g^2 to values higher than that of the noninteracting ideal molecule (R_0^2). This must be done while preserving the connectivity of the dendrimer. We found that the effective step length l_1 may be estimated from the solution of the cubic equation given in reference 25 and in the Supporting Information. The number of effective segments N_1 is found by requiring that the contour length L of the molecule remain fixed under the rescaling operation. Thus, $N_1 = (N - 1)l_0/l_1 + 1$, where l_0 is the bare step length. With these two rescaled values, the behavior of the dendrimer in the presence of an external perturbation may be estimated with a much simpler model and $R_g^2 \equiv R_0^2$.

Following de Gennes, we write the Flory free energy density as a function of the perpendicular component of the radius of gyration R_z for a single adsorbed dendrimer in a layer composed of N_d molecules: $F/kT \propto (R_0/R_z)^2 - wN_1f_s$. Unlike the scenario involving linear chains, we are justified in considering a single dendrimer in the adsorbed layer since the high degree of branching limits the extent of interpenetration between different molecules. The first term on the right-hand side captures the compression of the dendrimer along the axis perpendicular to the plane. The second term counts the enthalpic gain due to dendrimer segments touching the charged surface. Given the high ionic strength (and, thus, charge screening) in the systems of interest, the enthalpy parameter w is treated as a simple numerical parameter dependent on surface charge. The fraction of dendrimer segments touching the surface f_s should vary as the ratio of a thin shell on the molecule's surface to its volume, l_1/R_z. One also expects that f_s is inversely proportional to the number of dendrimers in the layer N_d since fewer segments from each individual molecule would need to be recruited to neutralize the surface charge as more molecules isolate to the interface. The fraction should also increase with increasing w. Finally, unlike simple linear molecules, one may expect that the fraction of available segments within compact dendritic molecules varies with generation. Thus, f_s also depends on an inverse compressibility or "openness function" f_G that we approximate as the square ratio of the radius of gyration to the total contour length: $f_G \propto (R_g/L)^2$. Thus, we expect that the fraction of segments touching the surface $f_s \propto (wl_1/R_zN_d)(R_g/L)^2$.

Minimizing F/kT with respect to R_z leads to the relationship $R_z \propto N_dL/w^2$ in the weakly adsorbed limit, similar in form to the corresponding scaling law for linear chains in the plateau region of the adsorption isotherm. Some differences are notable, however. Unlike the ideal linear chain, the height above the plane for dendrimers varies as the inverse square of the enthalpy and directly depends on the number of dendrimers in the layer. The behavior of N_d is complicated and is likely dictated by an intricate balance between the dendrimers' ability to pack on the surface, the number of charges it carries, and the solution entropy. However, one may expect that an upper limit inversely proportional to R_g^2 will be reached due to packing constraints at the surface. Nevertheless, as discussed below and reported in the literature, standard adsorption isotherms successfully encapsulate the dendrimer solution's behavior over a broad range of concentrations. Similarly, one also expects that R_z reaches some limiting value below which it can no longer be compressed in the limit of strong adsorption.

To test these predictions, we performed molecular dynamics simulations of an electrolyte solution consisting of monocentric dendrimers and their attendant counterions placed between two model electrode surfaces. Every bead within the model dendrimers carries a unit positive charge. We examined the behavior of four different generations of growth, G, spanning G = 2, 3, 4, and 5. Each of the two electrode surfaces is modeled by a grid of 225 equally spaced immobile particles. Each particle is uniformly assigned a fixed positive or negative charge, depending upon the electrode, that is required to achieve a given surface charge density σ. Combined, the two electrodes form two planes at the top and bottom edges of the simulation box. The simulation box is periodic in the two lateral directions.

The basic length scale for the simulations is set by the Bjerrum length of water at 25 °C, l_w (roughly 7 Å). The spacing between electrode beads was fixed at l_w in a simple square lattice. The box dimensions are set to $15l_w \times 15l_w \times 15l_w$. Four different concentrations of electrolyte were examined for each value of G studied. Noting that a typical electrolyte employs a 1 M concentration of charged species, we need roughly 680 charged groups attached to the dendrimers within the simulation box to match a typical concentration c^*. We considered concentrations of approximately $0.5c^*$, c^*, $1.5c^*$, and $2c^*$. However, since the charges come in discrete quantities dependent upon G, the value of c^* varied slightly as a function of the generation of growth. Specifically, c^* corresponds to 68, 30, 14, and 8 dendrimers for generations 2, 3, 4, and 5, respectively. Eleven different surface charge densities were examined with $\sigma l_w^2 = 0.0-1.0$. We estimate w by a simple series expansion about σ: $w \propto 1/kT(|\sigma l_w^2| + a_2|\sigma^2 l_w^4|)$ where kT is the thermal energy. The unknown coefficient a_2 remains as a fitting parameter and is given a value of 0.25. Values for l_1 are estimated from simulations of electrolyte solutions between noncharged electrodes. All simulations were carried out with the LAMMPS[26,27] simulation code. Additional details on the simulation are given in the Supporting Information.

Figure 1 illustrates the model with typical snapshots from the simulations. The figure presents images taken from a $2c^*$ simulation of G = 5 dendrimers sandwiched between the electrodes. The reduced surface charge density σl_w^2 is 0.1 on the left and 1.0 on the right. The red beads belong to the dendrimer; the white beads are the counterions; and the gold beads compose the electrodes.

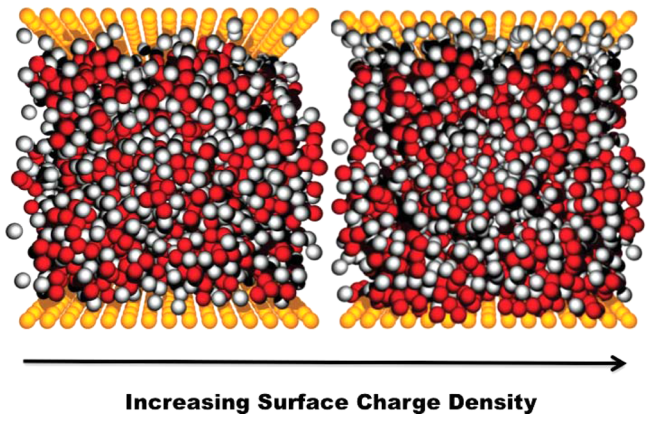

Figure 1. Snapshots from simulations of G = 5, $c = 2c^*$ configurations with $\sigma l_w^2 = 0.1$ on the left and $\sigma l_w^2 = 1.0$ on the right. The red beads represent the dendrimer; the white beads are the counterions; and the gold beads compose the electrodes.

dx.doi.org/10.1021/mz400524c | ACS Macro Lett. 2014, 3, 180−184

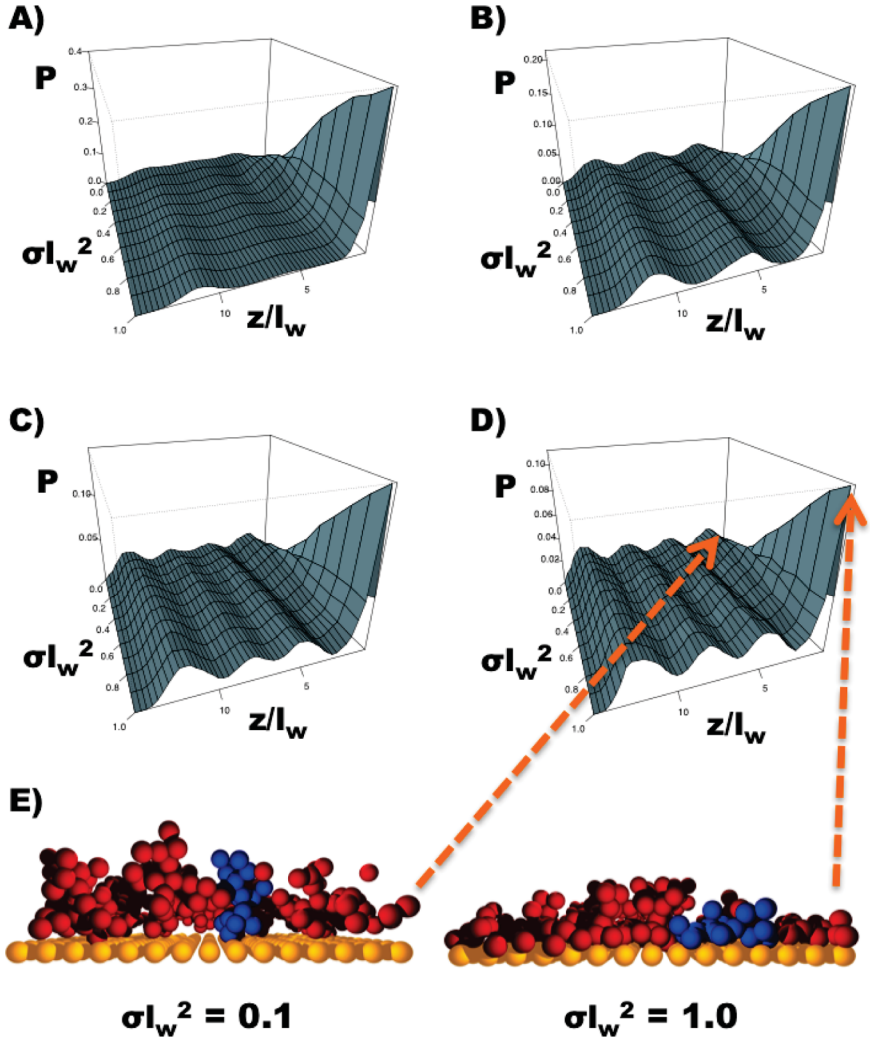

Figure 2. Probability P of finding a model segment along the perpendicular axis between the two electrodes as a function of reduced surface charge density σl_w^2. Plots for $G = 3$ and concentrations (A) $0.5c^*$, (B) c^*, (C) $1.5c^*$, and (D) $2c^*$ are shown. In part (E), snapshots of those dendrimers touching the electrode are shown for $G = 3$ and $c = 2c^*$ at high and low surface charge densities. The arrows indicate the approximate location of each snapshot on the probabilty plot given in part D. One dendrimer in each snapshot is highlighted in blue to demonstrate the flattening of individual molecules within the adsorbed layer.

As suggested by Figure 1, the mass distribution between the electrode plates depends upon the charge density, as well as other factors such as concentration and generation of growth. To probe the impact of these variables, we calculate the probability $P(z)$ of finding dendrimer or counterion segments at locations perpendicular to the electrode surfaces. Specifically, $P(z) = n(z)/n_T$ where $n(z)$ is the number of particles found to fall over the course of the simulation between $z \pm dz$, with a bin width of $dz = 0.3l_w$, and n_T is the sum over the value of $n(z)$ for all bins. Figure 2 presents $P(z)$ for the dendrimer segments for $G = 3$ over a range of σl_w^2 and c values. The concentrations increase moving from (A) to (D) in the figure. The rightmost portion of each surface plot (lowest value of z/l_w) corresponds to the electrode with opposite charge to the dendrimer, while the similarly charged electrode lies left (highest value of z/l_w). The back plane represents the neutral $\sigma l_w^2 = 0$ simulation, and the highest value of σl_w^2 falls in the foreground. Several notable features are evident. First, several maxima exist as a function of z/l_w for all values of σl_w^2. Their number increases as the concentration increases, as expected. For all values of surface charge density, the space near the similarly charged electrode is avoided by the dendrimer, creating a depletion layer. As the surface charge increases, however, the oppositely charged electrode accumulates significant dendrimer density at the expense of the closest maxima found in the lower charge density simulations. At the lower concentrations, the dendrimers move slightly closer to the oppositely charged plane, participating in a double layer with the counterions. The counterion probability map mirrors that of the dendrimer but is less well-defined in the bulk (see the Supporting Information for details). Similar plots are found for most combinations of G, σ, and concentration studied. That the most proximate density peak moves closer to the substrate surface provides the key observation for the discussion herein. This observation indicates that the simulations cover surface charge densities that result in perturbation of only the first layer of dendrimers closest to the surface. Details of the double layer structure and potential drop across the two electrodes will be reported in a later study.

As charge builds on the electrode, one may imagine three scenarios for how additional dendrimer charges add to the interface. The dendrimers may deform, pressing more of their

dx.doi.org/10.1021/mz400524c | *ACS Macro Lett.* 2014, 3, 180−184

segments to the surface; more dendrimers may add to the interface; or some combination of addition and deformation may take place. Part E of Figure 2 illustrates that flattening certainly takes place. To determine which of these specific possibilities is realized and to compare with the simple scaling argument provided above, we calculate the average number of discrete dendrimers N_d that have at least one segment in contact with the oppositely charged electrode. Contact is defined as falling within two bead diameters from the midplane of the electrode. We find that a simple second-order Langmuir isotherm (with minor modification) captures the dependence of N_d on the binding enthalpy and concentration, similar to experimental findings.[11,18,28] Specifically, we find that $N_d 2\pi R_g^2/A \propto (i_1 \exp(w)c + 2i_2 \exp(w)c^2)/(1 + i_1 \exp(w)c + i_2 \exp(w)c^2) + i_0 \equiv I_L(c,w)$. The term on the left reflects the drive toward a terminal value of $N_d \propto A/R_g^2$ where A is the area of the attractive surface. The first term on the right is the familiar Langmuir isotherm with coefficients $i_1 = 0.4$ and $i_2 = -2 \times 10^{-5}$. Here, c is simply the number of dendrimers in the fixed-volume simulation box. Note that we have here assumed that the enthalpic gain on contact dominates the entropic loss. The last term in the isotherm reflects the changing ionic strength of the solutions with changing concentration; at lower concentrations of dendrimers, the molecules begin to add earlier than predicted by the simple isotherm but otherwise conform to the standard expression. Thus, $i_0 = 0.1$ for the lowest concentration studied and zero for the remaining three. For convenience, we define the modified second-order expression to be $I_L(c,w)$. Figure 3 presents the observed adsorption isotherms for all four concentrations studied and for generations $G = 2-4$. As evident in the $G = 4$ data, the finite size of the electrodes begins to lead to poor sampling statistics for the larger two generations of growth. Thus, though $G = 5$ follows the same form of isotherm, those results are not shown because the scatter confuses the

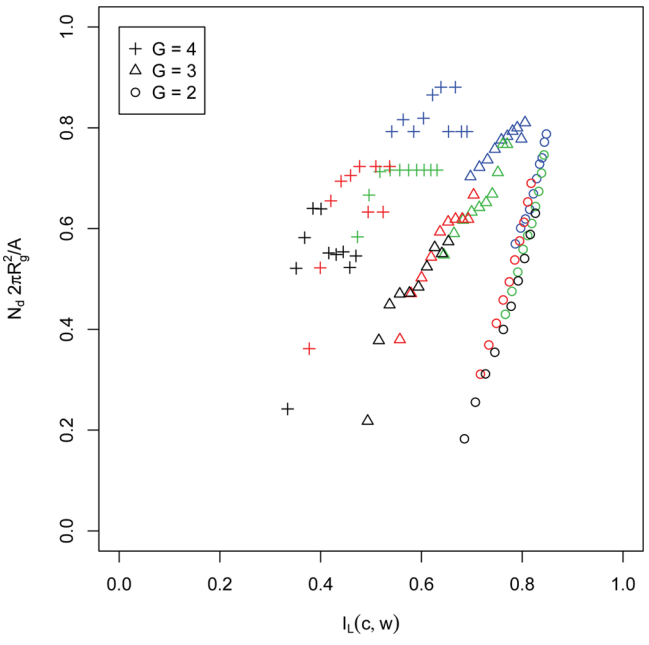

Figure 3. Average number of discrete dendrimers touching the oppositely charged electrode N_d, presented as the Langmuir isotherm described in the text. The colors encode concentration with black, red, green, and blue corresponding to $0.5c^*$, c^*, $1.5c^*$, and $2.0c^*$, respectively.

picture presented by the lower three generations. The data clearly demonstrate that, as one would expect, fewer dendrimers of higher generation are needed to achieve charge neutrality compared against their smaller counterparts.

The isotherms suggest continued addition to the surface with increasing attraction. However, this tells only a portion of the story. We also must consider the fraction of segments within a dendrimer that are bound to the surface f_s to determine which of the proposed scenarios is active. As in the estimation of N_d, segments found to lie within a distance of two bead diameters from the attractive electrode midplane are counted as touching the surface. Figure 4 presents these estimates for all

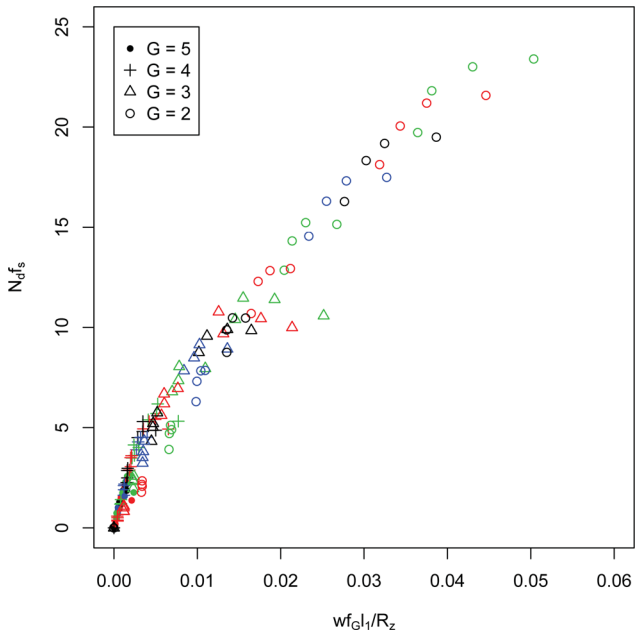

Figure 4. Number of dendrimer segments $N_d f_s$ in contact with the oppositely charged electrode normalized by the predicted scaling as a function of the enthalpy gained on contact with the surface w_s, plotted in accord with the predicted scaling.

concentrations and generations of growth studied, in terms of the scaling prediction above. Clearly, the scaling estimate works well, but two different regimes are evident. At low values of attraction (small w), the fraction of dendrimer segments on the surface that are in contact with the electrode $N_d f_s$ rapidly rises. This quantity then rolls over into a regime in which the number of segments grows more slowly but is still in accord with the predicted scaling. Some generational dependence can be discerned, with lower generations tending to fall predominantly in the regime with slower segment growth. Comparison of the number of segments adsorbed to the surface charge suggests a tendency to overcharge the surface over the range of σ values studied. However, the exact values of N_d and f_s are subject to the chosen distance threshold, and future study of the double layer is merited.

This addition of segments coincides with compression of the dendrimers against the surface. Figure 5 contains two plots of the component of the radius of gyration perpendicular to the surface, R_z, averaged over all of the bound dendrimers. In the main plot, estimates for all of the generations of growth G, adsorption enthalpies w, and concentrations are presented in a form that illustrates the transition from compressed to noncompressed. The ratio of R_z to the total root-mean-squared

dx.doi.org/10.1021/mz400524c | ACS Macro Lett. 2014, 3, 180−184

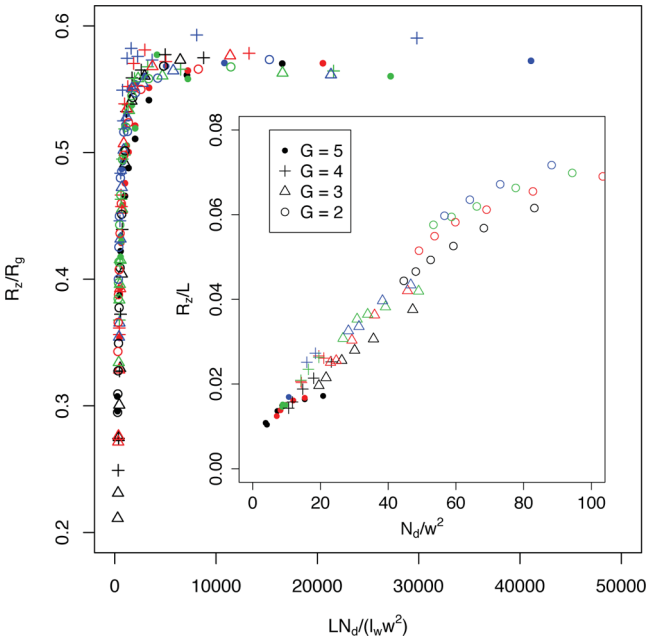

Figure 5. Component of the root-mean-square radius of gyration along the axis perpendicular to the electrode R_z as a function of the inverse enthalpy of contact, normalized as prescribed by the predicted scaling.

radius of gyration R_g rises rapidly as the surface charge density decreases and then asymptotes to the expected value of roughly 0.58 for noncompressed molecules. From this, we see that compression occurs below a threshold value of LN_d/w^2. The insert plot presents the data in the form of the predicted scaling law derived above. However, for clarity, only data for $R_z/R_g < 0.49$ (that is, only data in the compressed region of the main plot) are shown. Here, we see that the proposed scaling works well; the height of the layer formed by the adsorbed dendrimers varies directly with the number of dendrimers adsorbed N_d and the total contour length of the dendrimers L while changing in proportion to the inverse of the squared enthalpy.

In summary, we present herein a simple scaling argument that captures many of the salient features of the phenomena at interfaces between charged surfaces and concentrated dendrimer solutions. Those predictions appear to agree well with extensive molecular dynamics simulations that span a range of concentrations, electrode surface charges, and dendrimer generation of growth. From these results, we conclude that charge on the substrate is satisfied by a combination of addition of dendrimers to the surface and concurrent compression of the molecules against the substrate. We appeal to two key assumptions. First, we use an effective model for the dendrimer that captures its internal repulsions by rescaling the effective step length between segments. This quantity may be estimated from the radius of gyration of the free dendrimer. Second, we assume weak adsorption in which only the first layer of dendrimers near the surface is affected by the charge on the electrodes. These results should yield to direct experimental evaluation and may be of use in designing new chemistries for advanced applications.

■ ASSOCIATED CONTENT

Ⓢ Supporting Information

The expressions used for estimating the effective step length l_1, the details of the simulations, and typical plots of the ion distributions and net charge densities are provided. This material is available free of charge via the Internet at http://pubs.acs.org.

■ AUTHOR INFORMATION

Corresponding Author

*E-mail: pwelch@lanl.gov.

Notes

The authors declare no competing financial interest.

■ ACKNOWLEDGMENTS

This work was carried out under the auspices of the National Nuclear Security Administration of the U.S. Department of Energy at Los Alamos National Laboratory under Contract No. DE-AC52-06NA25396. Financial support provided by the Los Alamos National Laboratory Directed Research and Development program. Computing time was provided by Los Alamos National Laboratory's Institutional Computing.

■ REFERENCES

(1) Helms, B.; Meijer, E. W. *Science* **2006**, *313*, 929.
(2) Astruc, D. *Nat. Chem.* **2012**, *4*, 255.
(3) Dobrynin, A. V.; Rubinstein, M. *Prog. Polym. Sci.* **2005**, *30*, 1049.
(4) Ondaral, S.; Wågberg, L.; Enarsson, L.-E. *J. Colloid Interface Sci.* **2006**, *301*, 32.
(5) Striolo, A.; Prausnitz, J. M. *J. Chem. Phys.* **2001**, *114*, 8565.
(6) Suman, B.; Kumar, S. *J. Phys. Chem. B* **2007**, *111*, 8728.
(7) Voulgarakis, N. K.; Rasmussen, K.Ø.; Welch, P. M. *J. Chem. Phys.* **2009**, *130*, 155101.
(8) Lenz, D. A.; Blaak, R.; Likos, C. N. *Soft Matter* **2009**, *5*, 2905.
(9) Lewis, T.; Ganesan, V. *J. Phys. Chem. B* **2013**, *117*, 9806.
(10) Tsukruk, V. V.; Rinderspacher, F.; Bliznyuk, V. N. *Langmuir* **1997**, *13*, 2171.
(11) Takada, K.; Diaz, D. J.; Abruña, H. D.; Cuadrado, I.; Casado, C.; Alonso, B.; Morán, M.; Losada, J. *J. Am. Chem. Soc.* **1997**, *119*, 10763.
(12) Esumi, K.; Goino, M. *Langmuir* **1998**, *14*, 4466.
(13) Bliznyuk, V. N.; Rinderspacher, F.; Tsukruk, V. V. *Polymer* **1998**, *39*, 5249.
(14) Tokuhisa, H.; Zhao, M.; Baker, L. A.; Phan, V. T.; Dermody, D. L.; Garcia, M. E.; Peez, R. F.; Crooks, R. M.; Mayer, T. M. *J. Am. Chem. Soc.* **1998**, *120*, 4492.
(15) Hierlemann, A.; Campbell, J. K.; Baker, L. A.; Crooks, R. M.; Ricco, A. J. *J. Am. Chem. Soc.* **1998**, *120*, 5323.
(16) Mecke, A.; Lee, I.; Baker, J. R.; Banaszak Holl, M. M.; Orr, B. G. *Eur. Phys. J. E* **2004**, *14*, 7.
(17) Lojou, E.; Bianco, P. *Bioelectrochemistry* **2006**, *69*, 237.
(18) Schlapak, R.; Armitage, D.; Saucedo-Zeni, N.; Latini, G.; Gruber, H. J.; Mesquida, P.; Samotskaya, Y.; Hohage, M.; Cacialli, F.; Howorka, S. *Langmuir* **2007**, *23*, 8916.
(19) Porus, M.; Clerc, F.; Maroni, P.; Borkovec, M. *Macromolecules* **2012**, *45*, 3919.
(20) Jachimska, B.; Łapczyńska, M.; Zapotoczny, S. *J. Phys. Chem. C* **2013**, *117*, 1136.
(21) Kłgos, J. S.; Sommer, J.-U. *Polym. Sci. Ser. C* **2013**, *55*, 125.
(22) Kröger, M.; Peleg, O.; Halperin, A. *Macromolecules* **2010**, *43*, 6213.
(23) de Gennes, P. G. *J. Phys. Paris* **1976**, *37*, 1445.
(24) de Gennes, P. G. *Scaling Concepts in Polymer Physics*; Cornell University Press: Ithaca, 1979.
(25) Welch, P. M. *J. Chem. Phys.* **2013**, *139*, 164906.
(26) Plimpton, S. *J. Comput. Phys.* **1995**, *117*, 1.
(27) http://lammps.sandia.gov. (Accessed Jan 24, 2013).
(28) Manríquez, J.; Juaristi, E.; Muñoz-Muñiz, O.; Godínez, L. A. *Langmuir* **2003**, *19*, 7315.